CALCULATION OF SEPARATED FLOWS BY MEANS OF BOUNDARY-LAYER EQUATIONS

V. I. Vasil'ev, S. V. Khokhlov, and E. Yu. Shal'man

UDC 532.526.2:532.526.4

The possibility of calculating separated flows by means of integral methods of boundary-layer theory was demonstrated in [1]. In [2], it was shown that by solving the inverse problem for the complete system of boundary-layer equations and taking into account interaction with the external flow, it is relatively simple to calculate flows with thin separated regions without having to resort to integration of the Navier–Stokes equations. This approach is now used mainly to describe flows around airfoils [3, 4]. The goal of the present investigation is to develop a computational method that, while staying within the framework of the theory of interacting boundary layers, would make it possible to calculate a somewhat different class of flows – flows that are frequently encountered in pratical applications. We are concerned in particular with flows in diffuser channels and channels in which two flows are separated. We will examine both laminar and turbulent flows. A method is proposed for speeding up the convergence of the iteration.

1. It should be noted that, in principle, there are several different ways to describe strong interaction (the latter being the main feature of separated flows). The methods can be classified according to criteria such as the type of problem (direct or inverse) that is solved for the external flow and the boundary layer. The first possiblity is a purely direct problem. Here, a determination is made of the velocity of the inviscid flow along the surface u_e. Then the displacement thickness δ is found and the contour of the surface is adjusted for this value. Finally, the value of u_e is calculated a second time. This process is continued until a steady-state is established and can be represented in the form of the scheme

$$u_e \to \delta \to u_e \to \delta \to \ldots \tag{1.1}$$

The second possiblity is a purely inverse problem. First we assign the displacement thickness. We determine the velocity on the external boundary U_e from the inverse problem for the boundary layer. This velocity should coincide with the velocity in the inviscid flow. To ensure satisfaction of the latter condition, we solve the inverse problem for the external flow and find the new distribution of δ, etc. This procedure can be represented schematically in the form:

$$\delta \to U_e \to \delta \to U_e \to \ldots \tag{1.2}$$

The third possibility is to solve an inverse-direct problem. We assign the distribution of u_e and find two displacement thicknesses: δ from the solution of the direct problem for the boundary layer and δ from the solution of the inverse problem for the external flow. The value of u_e is corrected on the basis of the difference of these two results and the process is repeated:

$$u_e \nearrow \delta \searrow \; u_e \nearrow \delta \searrow \cdots \qquad \Delta \qquad \Delta \tag{1.3}$$

Finally, we can examine a direct-inverse problem. Here, we specify the displacement thickness and find u_e (direct problem) and U_e (inverse problem for the boundary layer), then using the difference of the latter two quantities to correct δ:

Moscow. Translated from Zhurnal Prikladnoi Mekhaniki i Tekhnicheskoi Fiziki, No. 6, pp. 46-54, November-December, 1990. Original article submitted December 2, 1988; revision submitted May 10, 1989.

0021-8944/90/3106-0839$12.50

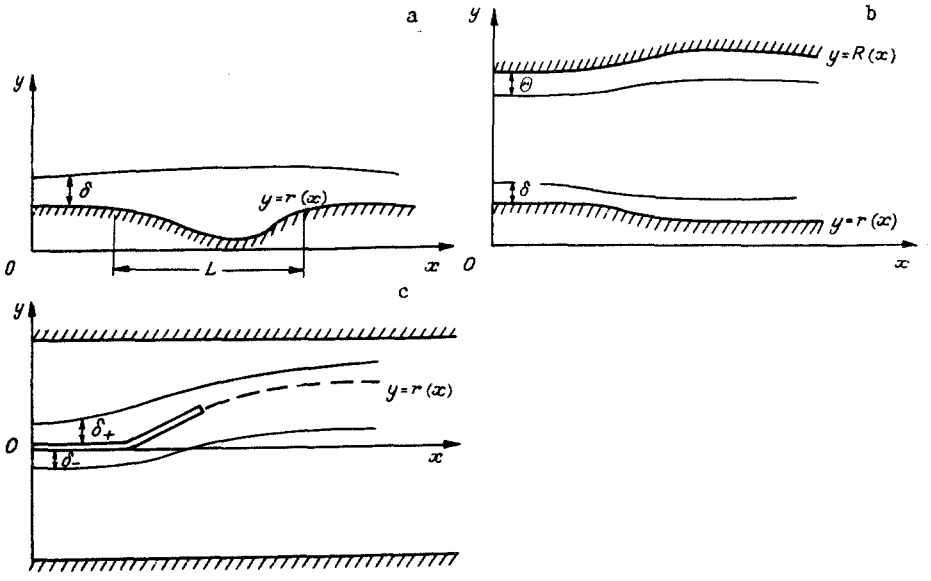

Fig. 1

$$\delta \overset{U_e}{\underset{u_e}{\rightleftarrows}} \delta \overset{U_e}{\underset{u_e}{\rightleftarrows}} \cdots \tag{1.4}$$

There are also other approaches, normally used within the framework of the three-deck model in [5]. The approaches represented by (1.1) and (1.3) involve the solution of a direct boundary-layer problem and, thus, the appearance of a Gol'dshtein singularity [5]. Thus, the solution of problems within the framework of these approaches requires the use of special procedures to avoid the appearance of singularities during numerical integration of the boundary-layer equations. Such procedures are usually not universal, and the iterative process often does not converge. The use of approach (1.2) involves the solution of an inverse problem for an inviscid flow. Obtaining such a solution is very difficult in certain cases – such as in channels – while there is a whole range of effective algorithms for solving direct problems in the case of inviscid flows. The approach which is currently most widely used to describe viscid/inviscid interaction is the direct-inverse approach (1.4). We will use this approach to construct our computing method as well.

2. Figure 1 shows sketches depicting plane flows of an incompressible fluid that we will be examining (a – flow past a free surface whose contour is described by the equation y = r(x); b – flow in a channel; c – motion of two flows with different total pressures past a divider installed in a channel). It is assumed that the Reynolds number Re is large and that the characteristic dimension of a nonuniformity on the surface over which the flow is travelling is on the order of the thickness of the boundary layer ($\Delta r = O(\delta)$. Thus, the separation zones will be thin. When we analyze the flow in the channel, moreover, we assume that there is an inviscid core and boundary layers. The transverse dimension of the core is on the order of the channel width R – r. In addition, $\delta \leq (R - r)$.

When these conditions are satisfied, the boundary layer is conveniently described in the variables

$$X = x,\ Y = y - r(x),\ U = u;\ V = v - u\,(dr/dx)$$

(x and y are cartesian coordinates (see Fig. 1); u and v are components of the velocity vector in these coordinates). The equations have the standard form in the new variables

$$U\partial U/\partial X + V\partial U/\partial Y = \beta + \partial((\nu + \varepsilon)\partial U/\partial Y)/\partial Y; \tag{2.1}$$

$$\partial V/\partial Y = -\partial U/\partial X. \tag{2.2}$$

Here, we have also introduced the notation; $\beta = U_e dU_e/dX$, $U_e(X) = \lim_{Y\to\infty} U(X, Y)$, , ν is laminar viscosity, ε is eddy viscosity. The latter quantity can be found by means of a semi-empirical model. It should be pointed out that the parameter β is not known beforehand in the inverse problem. To determine it, we must assign the distribution of the displacement thickness

$$\int_0^\infty (1 - U/U_e)\, dY = \delta(X). \tag{2.3}$$

The boundary conditions for system (2.1)-(2.2)

$$Y = 0 \;\; U = V = 0, \; Y \to \infty \;\; \partial U/\partial Y \to 0. \tag{2.4}$$

while the distribution of longitudinal velocity in the initial section must be specified

$$U(0, Y) = U_e(0)\, f(Y). \tag{2.5}$$

We assumed in the calculations that the initial section of the surface was a straight line r = const. In the laminar case, f(Y) was found from the Blausius solution. In the turbulent case, it was approximated by the velocity profile on a plate [6].

Problem (2.1)-(2.5) was solved numerically. Equation (2.1) was written in finite-difference form by means of the Crank–Nicolson scheme in central differences in the variable Y. The use of this scheme with a uniform grid ensured second-order approximation with respect to this coordinate. Since Eq. (2.1) is nonlinear, we used local (in each section) iterations to realize a second-order approximation with respect to X. In writing the convective terms in the region of reverse flow (U < 0), we used the approximation [7] $U\partial U/\partial X = 0$, if U < 0. In solving the problem of interaction in the reverse flow zone, for certain calcutions we approximate $\partial U/\partial X$ with differences directed counter to the flow. In this case, the missing values of U were taken from the previous calculation. The results obtained in the two cases were nearly the same, although the first method [7] requires less computing time. We took central differences for the discretization of (2.2), while the trapezoid formula was used in writing the integral (2.3). Thus, on the whole, the numerical method represented a second-order approximation.

Since the parameter β and the field U are both unknown in (2.1), finite-difference analogs (2.1) and (2.3) have to be solved together in any section. The corresponding system of difference equations has the form

$$a_j U_{j+1} - b_j U_j + c_j U_{j-1} = e_j \beta + d_j, \; 2 \leqslant j \leqslant N - 1; \tag{2.6}$$

$$\sum_{j=1}^{N} w_j U_j = 0; \tag{2.7}$$

$$U_1 = 0, \; U_N = U_{N-1}, \tag{2.8}$$

where the form of the coefficients has been omitted to save space; N is the number of grid points along Y. Equations (2.8) constitute a difference approximation of boundary conditions (2.4). To avoid additional iterations in the solution of system (2.6)-(28), we used a modification of the trial-run method

$$U_{j+1} = D_j U_j + G_j + E_j \beta. \tag{2.9}$$

Using the second boundary condition of (2.8) and relations (2.6) along with recursion formulas, we find the necessary correction factors. Inserting (2.9) into (2.7), we exclude U_j. Considering that $U_1 = 0$, we find β. We then use an inverse trial run and Eq. (2.9) to determine the field U. It is not hard to show that the sufficient conditions for stability (the conditions for a_j, b_j, c_j) for the modification of the trial-run method are the same as in the usual case [8].

Along with the method of solution described above, we also tried a variant in which, instead of problem (2.1)-(2.4), we examine an equivalent problem

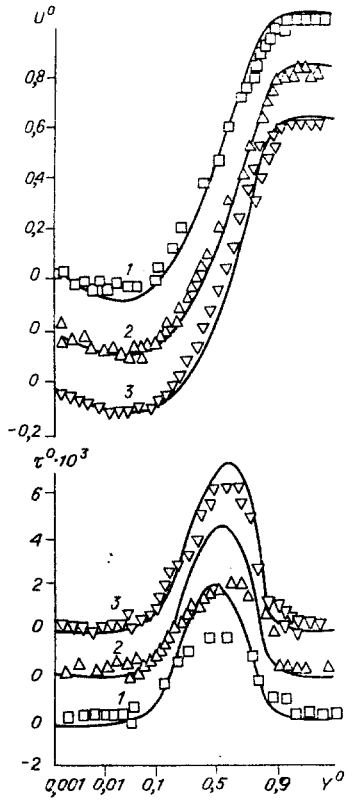

Fig. 2

$$U\partial\omega/\partial X + V\partial\omega/\partial Y = \partial^2((\nu + \varepsilon)\omega)/\partial Y^2; \tag{2.10}$$

$$\partial U/\partial Y = \omega; \tag{2.11}$$

$$\partial V/\partial Y = -\partial U/\partial X; \tag{2.12}$$

$$\int_0^\infty (Y - \delta)\,\omega dY = 0; \tag{2.13}$$

$$Y = 0 \quad U = V = 0, \; Y \to \infty \quad \omega \to 0. \tag{2.14}$$

As in the first case, when we use these difference schemes we find that it is necessary to solve the following system in the cross section

$$a_j\omega_{j+1} - b_j\omega_j + c_j\omega_{j-1} = d_j, \quad 2 \leqslant j \leqslant N - 1; \tag{2.15}$$

$$\sum_{j=1}^{N} w_j\omega_j = 0; \tag{2.16}$$

$$\omega_N = 0. \tag{2.17}$$

We used the standard trial-run formulas to solve system (2.15)-(2.17). However, since we had integral equation (2.16) in place of one of the boundary conditions, we found ω_1 by means of the same elimination method as was used to determine β. This approach provides the same degree of accuracy but saves somewhat on computer memory, since fewer correction factors need to be stored.

In most of the calculations presented below, the grid was uniform with respect to X, while the subdivision along Y was made denser toward the wall in accordance with the recommendations in [9]. It should be noted that when flows in channels are being examined, the corresponding problem must be solved for the boundary layer on each surface.

3. We described turbulent flows by means of the one-parameter model in [10]

$$U\partial\varepsilon/\partial X + V\partial\varepsilon/\partial Y = \partial((\varkappa\varepsilon + \nu)\partial\varepsilon/\partial Y)/\partial Y + \alpha\varepsilon|\partial U/\partial Y| - \gamma\varepsilon(\xi\varepsilon + \nu)/Y^2, \quad (3.1)$$

where $\varkappa$, γ, and ξ are coefficients; α is a function of the ratio ε/ν. The boundary conditions have the form

$$Y = 0 \quad \varepsilon = 0, \; Y \to \infty \quad \partial\varepsilon/\partial Y \to 0.$$

As the initial conditions, we asigned the distribution of eddy viscosity in the boundary layer on a flat plate [6]. For numerical integration of (3.1), we used the same finite difference scheme as for (2.1).

The model in [10] has been proven valid in many different cases and is particularly suited for calculations of attached boundary layers, mixing layers, and jets. To evaluate the accuracy of the description of separation, we examined the flow observed experimentally in [11]. We solved the inverse problem. Here, the distribution of $\delta(X)$ was borrowed from [11], while a comparison was made for theoretical and measured distributions of velocity and shear stress. In Fig. 2, velocity is referred to the velocity in the given section ($U^0 = U/U_e(X)$); the shear stresses τ are referred to the velocity head ($\tau^0 = \tau/\rho U_e^2(X)$); the longitudinal coordinate is referred to the quantity L, which is equal to the distance from the inlet to the model to the last section in which measurements were made (L = 508 cm), ($X^0 = X/L$, $Y^0 = Y/\delta$). The points show the experimental results, while the curves show the calculated results: $X^0 = 0.694$ (1), 0.724 (2), 0.782 (3). The coefficients in Eq. (3.1) were taken from [10] and were not specially corrected. Nevertheless, the model satisfactorily describes the distribution of the parametes in the separation zone.

4. The inviscid external flow is assumed to be a potential flow, i.e., if we introduce the function ψ, it should satisfy the Laplace equation:

$$\partial^2\Psi/\partial x^2 + \partial^2\Psi/\partial y^2 = 0. \quad (4.1)$$

To solve the problem on the interaction of the boundary layer with the external flow, it is sufficient to know the distribution of the velocity of the inviscid flow (u_e) along a contour corrected for the displacement thickness (such as at $y = r + \delta$ (see Fig. 1a)). It should be noted that only when this method of determining u_e is used will its combination with longitudinal velocity in the boundary layer also ensure combination with the transverse components. In problems concerning flow past a free surface, by using the theory of thin bodies it is possible to represent u_e in the form of an integral [2]

$$u_e(x) = W(x) + \frac{1}{\pi}\int_{-\infty}^{\infty} (d/d\xi\,(U_e\delta))/(x - \xi)\,d\xi, \quad (4.2)$$

where $W(x) = u_\infty + \frac{1}{\pi}\int_{-\infty}^{\infty} (dr/d\xi)/(x - \xi)\,d\xi$; u_∞ is the velocity of the incoming flow. With an assigned displacement thickness, Eq. (4.2) makes it possible to find $u_e(x)$. In numerical calculations, the integrals are taken over a finite segment outside of which $dr/dx = 0$. Also, it is possible to ignore the contribution of $d\delta/dx$ in this case. The size of this region should be determined from the condition of the independence of the results from the limits of intregration.

In a channel, calculation of $u_e(x)$ requires the solution of (4.1). Here, it is convenient to change over to the variables

$$\xi = x, \; \eta = [y - (r + \delta)]/[(R - \Theta) - (r + \delta)]$$

(R and r are the contours of the top and bottom walls (see Fig. 1b); θ and δ are the corresponding displacement thicknesses). As the boundary conditions, we assign the distribution of the stream function at the inlet and the upper and lower boundaries. At the outlet we impose the condition $\partial\Psi/\partial\xi = 0$, which gives a linear distribution of v and ensures that the solutions can be combined in the outlet section. In all of the calculations we performed, the flow at the inlet was assumed to be uniform, i.e., $\Psi = u_\infty(y - r - \delta)$ at x = 0, while

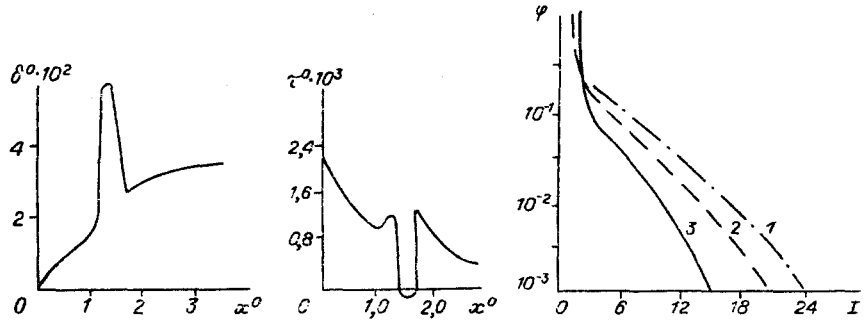

Fig. 3

the conditions of nonflow at $y = r - \delta$ and $y = R - \Theta$ had the form $\Psi = 0$ and $\Psi = Q$ (Q is the total discharge through the channel).

Finite difference analog (4.1), written in accordance with a second-order approximation scheme, was integrated by the iterative method of variable directions [8].

5. To combine the solutions in the boundary layer and the external flow, we need to satisfy the condition $U_e(x) = u_e(x)$. This allows us to find the displacement thickness. However, U_e and u_e functionals of δ whose explicit form is unknown. This compels us to use the iterative approach (1.4) to solve the direct-inverse problem. The organization of the iterations is a very important element of the method of calculation, and the overall volume of computation that is needed depends to a significant extent on the efficiency of this algorithm.

A simple iteration formula was proposed by Carter in [2]

$$\delta_{i+1}/\delta_i = 1 + \zeta((u_e - U_e)/U_e)_i \tag{5.1}$$

(i is the number of the iteration; ζ is the relaxation parameter). It is not possible to make an a priori estimate of ζ. An acceptable value of this quantity is chosen during calculations, which diminishes the efficiency of the method. We attempted to formulate a more effective and more reliable algorithm which speeds up the convergence of the process (1.4).

The integral in (4.2) is approximated in accordance with the trapezoid formula

$$u_m = W_m + \sum_{k=1}^{M} C_{km} U_k \delta_k. \tag{5.2}$$

Here, for brevity we have omitted the form of the coefficients C_{km} and dropped the index e in the velocity notation; k and m are the numbers of grid points along x; M is the total number of grid nodes. Analyzing the integral momentum equation for the boundary layer, we obtain an approximate relation which is valied in each section x:

$$\Delta U/U = -(\Delta\delta/\delta)/(2 + H) \tag{5.3}$$

($\Delta U = U_{i+1} - U_i$, $\Delta\delta = \delta_{i+1} - \delta_i$, H is the form factor). Finally, having required satisfaction of the $U_{i+1} = U_i$, we can use (5.2)-(5.3) to obtain a system of linear algebraic equations to find corrections to the displacement thickness

$$(u - U)_m = \sum_{k=1}^{M} \Gamma_{mk} \Delta\delta_k. \tag{5.4}$$

Having solved system (5.4) by the Gauss elimination method with isolation of the principal element, we find the new distribution of δ:

$$\delta_{i+1} = \delta_i + \zeta\Delta\delta. \tag{5.5}$$

The parameter ζ was taken equal to 0.5 in all cases. It should be noted that although we derived (5.4) with the use of Eq. (4.2) – which is valid for free flow – this iteration formula can actually also be used for calculations of flows in channels.

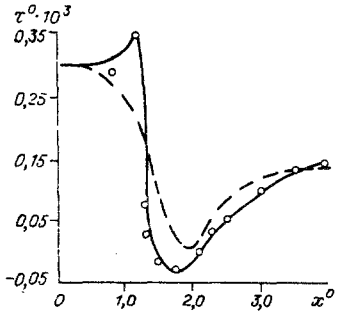

Fig. 4

The efficiency of the method was checked using the example of flow past a depression on a surface (see Fig. 1). The form of the depression was described by the relation $r(x)/L = 0.05[4(x^0 - 1.5)^2 - 1]^3$ with $1 \leqslant x^0 \leqslant 2$, $r(x) = 0$, $x^0 > 2$, $x^0 < 1$, where $x^0 = x/L$. Here, L is the depth of the depression. The flow in this case is laminar, and $\Delta x^0 = 1$. The point at which the boundary layer begins is located the distance $\Delta x^0 = 1$ from the depression. Figure 3 shows the distributions of the displacement thickness ($\delta^0 = \delta/L$) and friction on the wall $\left(\tau^0 = \tau_w/\rho u_\infty^2\right)$. It is evident that there is a separation zone. Also shown in the figure are the dynamics of the convergence of the iterations, $\varphi = |(u_e - U_e)/U_e|$; I is the number of the iteration; 1 shows the results it calculations with Eq. (5.1) for $\zeta = 0.5$; 2 shows the same when $\zeta = 1.2$; 2 shows the results obtained by the proposed method (5.4)-(5.5). If we use (5.1), then convergence does not occur when we attempt to assign ζ greater than 1.2, i.e., curve 2 turns out to be close to the limiting convergence curve. It is clear from this that the use of (5.4)-(5.5) actually speeds up convergence by at least 30%. We subsequently used only this approach to calculate free flows and flows in channels (see Fig. 1a and b).

6. To evaluate the possibility of calculating different flows in the channel, we examined two situations. 1. Laminar flow in a symmetrical diffuser channel ($R(x) = -r(x)$, $R(x)/L = 1 + 0.08(x^0 - 1)^2(5 - 2x^0)$ at $1 \leqslant x^0 \leqslant 2$; $R(x) = 1$ at $x^0 \leqslant 1$; $R(x) = 1.08$ at $x^0 \geqslant 2$; $x^0 = x/L$; ; L is the length of the transitional section). Such a flow was calculated in [12] by means of parabolized Navier–Stokes equations. 2. Turbulent flow in an asymmetric diffuser channel ($R/L = 0.75; r(x)/L = 0.201 - 1.981(x^0)^3 + 2.956(x^0)^4 - 1.176(x^0)^5$ at $0 \leqslant x^0 \leqslant 1$, $r(x)/L = 0.201$ at $x^0 \leqslant 0$, $r = 0$ at $x^0 > 1$). This type of flow was studied experimentally in [13].

In the first case $\mathrm{Re} = u_\infty L/\nu = 6{,}25 \cdot 10^3$, the boundary layer developes from a point located the distance $\Delta x^0 = 2.96$ from the transitional section. In the calculation, the initial section was placed at the distance $\Delta x^0 = 1$ from the transitional section. The distribution of friction on the channel wall is shown in Fig. 4 $\left(\tau^0 = \tau_w/\rho u_\infty^2\right)$: the solid line shows the results of the present study, while the points show data from [12]. It is evident that the two sets of results agree well with one another. Shown along with this information is the result of calculations performed within the framework of a parabolic approximation (dashed curve).

In the parabolic approximation, the boundary-layer equations were used to describe the entire flow field, while pressure was assumed to have been constant across the channel. Here, the size of the separation zone is reduced by a factor of 3 and, as is shown by other comparisons, has an error of up to 10% in the determination of the pressure gradient. Thus, when examining separated flows in a channel, it is important to consider the interaction of the boundary layer with the inviscid core. Then the boundary-layer approximation will provided a good description of the flow.

The turbuelent flow in the asysmmetric diffuser is characterized by $\mathrm{Re} = 5.85 \cdot 10^5$. The boundary layer develops from a point located the distance $\Delta x^0 = 2.7$ from the transitional section. The initial section was placed the distance $\Delta x^0 = 1$ from the transitional section. Figure 5 shows the distributions of friction on the undeformed wall $\left(\tau^0 = \tau_w/\rho u_\infty^2\right)$ and the pressure at this surface ($c_p = 2(p - p_0)/\rho u_\infty^2, p_0$, where p_0 is the pressure at the beginning of the transitional section); the solid line shows the calculation, while the points show the experiment [13]. The distribution of friction in the separation region is described satisfactorily, although some divergence is seen on the acceleration section. In turn, the theoretical pressure in the separation zone is somewhat exaggerated. Nonetheless, on the whole the correspondence can be considered satisfactory. However, to improve the accuracy of the results, it will be necessary to improve the turbulence model [10]. Calculations of flows in

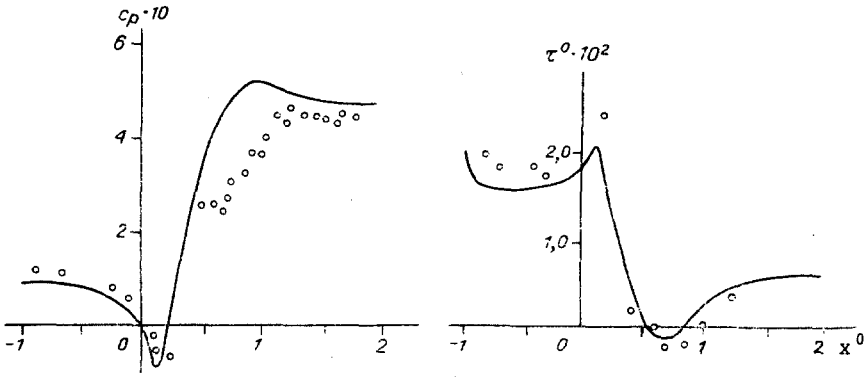

Fig. 5

channels were performed on grids containing 50 nodes along the x axis, 60 nodes along y in the boundary layer, and 20 nodes along y in the inviscid core. Computing time on an ES-1061 computer was roughly 5 min.

7. Finally one other type of flow which can be calculated in the approximation of an interacting boundary layer is flow past a divider installed in a channel (see Fig. 1c). The strong interaction of the boundary layer with the external flow near the trailing edge in this case is due both to an abrupt change in boundary conditions and to possible separation from the surface of the divider. An important difference between the given problem and the problem of flow past the trailing edge of an airfoil [4] is that the wake develops in channel. Also, the overall parameters (the Bernoulli constants in the incompressible fluid) may be different in the upstream and downstream flows. As a result of these circumstances, another parameter – the position of the wake – appears in the interaction problem.

As a line characterizing the position of the wake, we introduce a separating streamline ($y = r(x)$) which continues the surface in the flow to the trailing edge ($x = z$). We designate the displacement thickness of the boundary layer and the wake as δ_+ above this line and as δ_- below it. The flow is calculated in the following manner. With assigned δ_+, δ_-, and r, we independently determine the inviscid flows in the top and bottom halves by the same method as for a separate channel. In the region $x \leq z$ we solve two inverse problems (2.1)-(2.5) for boundary layers with assigned δ_+ and δ_-. In the region $x > z$, it is also possible to solve problem (2.1)-(2.5) for the upper and lower parts of the wake. However, here it is necessary to replace the attachement boundary condition by the condition of continuity of the velocity field on the separating streamline

$$Y = 0 \quad [U] = 0, \quad [\partial U/\partial Y] = 0, \; V = 0, \; \beta_+ = \beta_-, \tag{7.1}$$

where [...] denotes a discontinuity of a parameter. By virtue of the last condition of (7.1), we can assign only one of the quantities δ_+ or δ_-, from the side of the divider on which separation occurs (i.e., in the scheme depicted in Fig. 1c we assign δ_-).

Two combination conditions $(U_e)_+ = (u_e)_+$, $(U_e)_- = (u_e)_-$ make it possible to determine δ_+ and δ_- in the region $x \leq z$ and δ_- and r in the region $x > z$. The corresponding iterative algorithm is a generalization of the Carter algorithm. Thus, we use (5.1) at $x \leq z$, while at $x > z$

$$(\delta_-)_{i+1}/(\delta_-)_i = 1 + \zeta_1((u_- - U_-)/U_-)_i + \zeta_2((u_+ + U_+)/U_+)_i,$$
$$r_{i+1}/r_i = 1 + \chi_1((u_- - U_-)/U_-)_i + \chi_2((u_+ + U_+)/U_+)_i.$$

Convergent solutions are obtained at $\rho_1 = 1.0$; $\rho_2 = 0$; $\chi_1 = 0$; $\chi_2 = 0.1$. It is difficult to generalize algorithm (5.4)-(5.5) because there is no explicit expression for the dependence of δ_+ on δ_-.

As an example, we examined laminar flow past a divider whose form is described by the relation $r(x)/L = 1 + \tan \alpha(x^0 - 0.9)$ at $0.9 \leqslant x^0 \leqslant 1.9$, and $r(x)/L = 1$ at $x^0 \leq 0.9$. Here $x^0 = x/L$. The quantity L is the length of the deflected part. The value of $\alpha = 5°$. The sudden change in the contour of the parallel-walled channel at $x^0 = 0.9$ is smoothed with a radius of curvature equal to unity. The boundary layers on the divider develop from

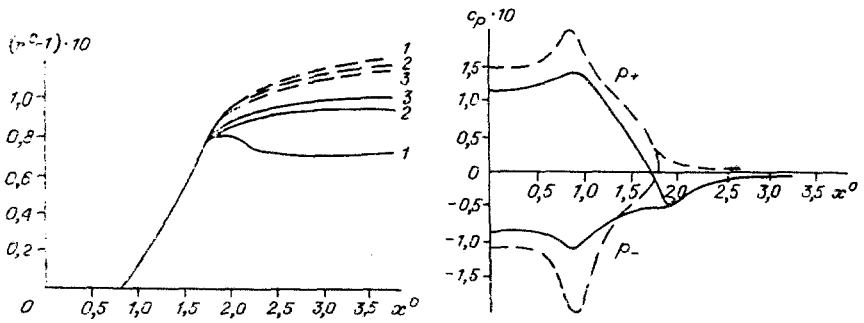

Fig. 6

a point located the distance $\Delta x^0 = 3.01$ from the trailing edge. The boundary layers on the walls of the channel were not taken into account. The value of $Re = 10^4$. We varied the ratio of the velocities at the inlet to the upper and lower parts of the channel $(m = (u_\infty)_+/(u_\infty)_-)$, there having been a proportionate change in Re_+ (at m = 1, $Re_+ = Re_-$). Figure 6 shows the positions of the separating streamlines ($r^0 = r/L$) at m = 0.05 (1), 1.0 (2), and 2.0 (3). The dashed lines show the corresponding results for the inviscid flow. Also shown is a comparison of the distributions of pressure $(c_p = (p - p_0)/\rho(u_\infty)_+^2$, where p_0 is the pressure at the outlet of the channel) in the inviscid and viscid flows at m = 1.0. In the inviscid flow, the position of the separating line depends weakly on m. Separtion is seen in the viscid flow near the trailing edge. The intensity of this separation increases with a decrease in m. The separating line is heavily deformed near the edge in this case. Rarefaction is seen in the viscous flow near the edge. This situation is interesting because it is possible to control the separation of one flow by changing the conditions in the other flow.

The results presented above show that the computing method used here to integrate the equations of an interacting boundary layer makes it possible to efficiently calculate a number of separated flows that are of practical interest.

LITERATURE CITED

1. L. V. Gogish and G. Yu. Stepanov, Turbulent Separated Flows [in Russian], Nauka, Moscow (1979).
2. J. E. Carter, "Solutions for laminar boundary layers with separation and reattachment," AIAA Paper, No. 583 (1974).
3. H. McDonald and W. R. Briley, "A survey of recent work on interacting boundary-layer theory for flow with separation," in: Numerical and Physical Aspects of Aerodynamic Flows. Vol. II, Springer, New York—Berlin (1984).
4. V. N. Vatsa and J. M. Verdon, "Viscid/inviscid interaction analysis of separted trailing-edge flows," AIAA J., 23, No. 4 (1985).
5. Aerodynamic Theory of Separated Flows [in Russian], Nauka, Moscow (1987).
6. J. O. Hinze, Turbulence, McGraw-Hill, New York (1959).
7. T. A. Reyhner and I. Flugge-Lotz, "The interaction of a shock wave with a laminar boundary layer," Int. J. Non-Linear Mech., 3, No. 2 (1968).
8. A. A. Samarskii, Theory of Difference Scheme [in Russian], Nauka, Moscow (1977).
9. J. Blotner, "Difference scheme with a nonuniform grid to calculate turbulent boundary layers," in: Numerical Solution of Problems of Fluid Mechanics [Russian translation], Mir, Moscow (1977).
10. G. N. Abramovich, S. Yu. Krasheninnikov, and A. P. Sekundov, Turbulent Flows in the Interaction of Body Forces and Non-Similitude [in Russian], Mashinostroenie, Moscow (1975).
11. R. L. Simpson, Y. T. Chew, and B. G. Shivaprasad, "The structure of separating turbulent boundary layer. Pt. I. Mean flow and Reynolds stresses," J. Fluid Mech., 113, 23 (1981).
12. A. Halim and M. Hafez, "Calculation of separation bubbles using boundary-layer type equations," AIAA J., 24, No. 4 (1986).
13. J. M. Serpa, R. C. Lessman, and W. M. Hagist, "Turbulent separated and reattached flows over a curved surface," AIAA Paper, No. 1064 (1985).